Motion Volume: Visualization of Human Motion Manifolds

Masaki Oshita
Kyushu Institute of Technology
Iizuka, Fukuoka,, Japan
oshita@ces.kyutech.ac.jp

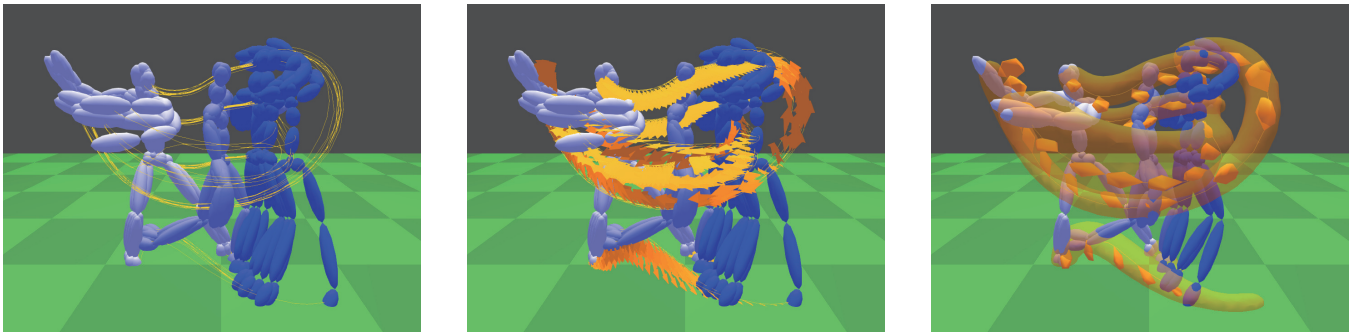

(a) input data (trajectories only) (b) input data (trajectories with orientations) (c) visualization (motion volumes)

Figure 1: Example visualization of the eight motions of a tennis forehand shot. (a)(b) The input data contain the spatial and orientational trajectories of body parts from a set of motions. (c) The output visualization contains the selected poses for key timings as well as spatial and orientational volumes for the body parts.

ABSTRACT

The understanding of human motion is important in many areas such as sports, dance, and animation. In this paper, we propose a method for visualizing the manifold of human motions. A motion manifold is defined by a set of motions in a specific motion form. Our method visualizes the ranges of time-varying positions and orientations of a body part by generating volumetric shapes for representing them. It selects representative keyposes from the keyposes of all input motions to visualize the range of keyposes at each key timing. A geometrical volume that contains the trajectories from all input motions is generated for each body part. In addition, a geometrical volume that contains the orientations from all input motions is generated for a sample point on the trajectory. The user can understand the motion manifold by visualizing these motion volumes. In this paper, we present some experimental examples for a tennis shot form.

VRCAI '19, November 14–16, 2019, Brisbane, QLD, Australia

ACM ISBN 978-1-4503-7002-8/19/11…$15.00
https://doi.org/10.1145/3359997.3365684

CCS CONCEPTS

• **Human-centered computing** → **Visualization techniques**; • **Computing methodologies** → *Motion processing*; *Volumetric models.*

KEYWORDS

Visualization, Human Motion, Motion Manifolds, Computational Geometry

ACM Reference Format:
Masaki Oshita. 2019. Motion Volume: Visualization of Human Motion Manifolds. In *The 17th International Conference on Virtual-Reality Continuum and its Applications in Industry (VRCAI '19), November 14–16, 2019, Brisbane, QLD, Australia.* ACM, New York, NY, USA, 7 pages. https://doi.org/10.1145/3359997.3365684

1 INTRODUCTION

The understanding of human motion is important in many areas such as sports, dance, and animation. In these areas, people often need to understand the variations in the motions of a specific form rather than just a single motion. For example, for a tennis trainee to practice a shot form, he or she needs to understand the manifold of the good motions rather than a single ideal motion because there are some variations even in the good motions that are performed by experts. However, because human motions are high-dimensional space-time data, it is difficult to visualize them in a way that people can easily understand. Playing back a motion clip as an animation is a common way to view a motion. However, because only one pose is displayed at a time during animation, it is difficult to understand the characteristics of the motion. To solve this problem, many methods

for depicting a motion as a single image have been developed [Assa et al. 2005; Bouvier-Zappa et al. 2007; Li et al. 2016; Yasuda et al. 2008]. However, these methods are intended for dealing with a single motion and cannot visualize the manifold of a motion form.

In this paper, we propose a method for visualizing the manifold of human motions. A motion manifold is defined by a set of motions in a specific motion form. Our method visualizes the ranges of the time-varying positions and orientations of a body part by generating volumetric shapes for representing them. It selects representative keyposes from the keyposes of all input motions to visualize the range of keyposes at each key timing. A geometrical volume that contains the trajectories from all input motions is generated for each body part. In addition, geometrical volume that contains the orientations from all input motions is generated for a sample point on the trajectory. The user can understand the motion manifold by visualizing these motion volumes. The generated three-dimensional (3D) shapes can be rendered as an image. The viewing position and orientation can be freely chosen by the user. An example of our results is shown in Figure 1. In this paper, we present some experimental examples for a tennis shot form.

The remainder of this paper is organized as follows. Section 2 review related work, Section 3 explains the input motion data, and Section 4 describes our method for generating motion volumes. Section 5 and 6 present the experimental results and discussion, respectively. Finally, Section 7 concludes the paper.

2 RELATED WORK

Because it is difficult for an observer to understand a motion when it is played back to him or her, many methods have been developed for depicting a motion as a single image [Cutting 2002; Li et al. 2016]. Drawing a series of important poses is one approach. Many methods have been developed for choosing important poses in a motion and drawing them. Assa et al. [2005] proposed a method for projecting a motion into a low-dimensional space to find important poses. Yasuda et al. [2008] proposed a method for drawing important poses on a timeline. The colors of the poses are determined by the direction in which they face. Bouvier-Zappa et al. [Bouvier-Zappa et al. 2007] proposed a method for adding visual cues to poses such as motion arrows, noise waves, and stroboscopic motion to represent the movements at each pose. These methods are intended to visualize one complex motion as an image and cannot be used to visualize a motion manifold that is defined by a set of motions.

Some methods have been developed for visualizing a large number of different motions [Hu et al. 2010; Jang et al. 2014; Sakamoto et al. 2004; Shen et al. 2017]. These methods are intended for categorizing the motions into groups and depicting the differences between them. Recently, Shen et al. [2019] proposed a metric for evaluating the similarity of motions in terms of the interaction between two characters or between a character and an object. These methods are also not suitable for visualizing motion manifolds.

The aim of most previous studies is to generate 2D images. In contrast, Zhang et al. [2018] proposed the MoSculp system, which generate 3D shapes for representing the trajectories of body parts from a motion sequence. They only depict the time-varying positions of body parts and cannot depict their time-varying orientations. Their method focuses on analyzing video for generating shapes. Moreover, their method is intended for a single motion and cannot be used to visualize motion manifolds. Kazi et al. [2016] developed a tool for creating 3D shapes that includes poses and visual effects representing movements. However, the 3D shapes must be authored by the user and they are not considered to represent motion manifolds. Our method also generates 3D shapes, but it is intended for representing the motion manifold of a set of motions, including not only the spatial but also the orientational ranges of body parts.

3 MOTION DATA

Our method takes a set of motions in a specific motion form as input. Instead of example motions, a generative statistical model [Lau et al. 2009; Min et al. 2009] that is constructed from a set of motions can also be used. Our method can take a number of example motions that are generated from such a statistical model.

Given a human body model, a pose is represented by the position and orientation of the pelvis as well as the rotations of all joints. A position is represented by a 3D vector. There are several ways to represent an orientation or rotation, such as a combination of rotational angles, 3×3 matrix, or quaternion. Our method works with any of these representations, so we used a 3×3 matrix in our implementation. A motion is represented by a series of poses. The positions and orientations of the body parts in any frame are computed based on the body model and pose using forward kinematics. The spatial and orientational trajectories of the body parts are represented by a series of positions and orientations, as shown in Figure 1 (b).

Our method assumes that the same number of key timings are specified for all the input motions. The key timings represent the important moments of the motions. For example, for the tennis forehand shot in Figure 1, three key timings were used: take-back, impact, and follow-through. These keyposes are commonly used in the training of tennis shot forms [Oshita et al. 2019]. The key timings can be either manually specified or automatically detected. To detect key timings, either some general methods such as [Assa et al. 2005] or motion-specific methods such as [Oshita et al. 2019] can be used. The appropriate number of key timings and method of detecting them depend on the target motion form and application.

We assume that all input motions are based on the same body model. In theory, motions from different body models can be treated together by applying a motion retargeting [Baek et al. 2003], as long as the difference is acceptable. However, motion retargeting is not explored in this paper.

We use only skeletal motions and do not use a skinned shape model. A pose can be drawn by using a stick figure with thickness parameters. Alternatively, a skinned shape model can be used for depicting poses, which may improve the visual quality. However, it highly depends on the quality of the skinned shape model, and making such a model for each set of motions is time consuming. Therefore, the use of a skinned shape model is not explored in this paper.

4 MOTION VOLUME GENERATION

4.1 Overview

This section describes our method for generating geometrical model for a motion manifold. The positions and orientations of body parts at each frame of each motion can be computed from the pose of the frame using forward kinematics. Our method generates shapes to represent the ranges of each keypose as well as the spatial and orientational ranges of each body part. Although the motion volumes can be generated for all body parts, in this paper, they are generated for the primary body parts: the pelvis, chest, head, right and left hands, and right and left feet, as shown in Figure 1. In practice, the body parts for which motion volumes are generated can be chosen depending on the target motion form and application.

Our method generates static shapes for visualizing this information and does not visualize temporal information. Neither the times of the sampling poses and points nor the spatial and rotational velocities of the body parts are considered. Although it is possible to use the colors of shapes for representing the temporal information, this is not explored in this paper. Because our method generates geometrical shapes and does not use their colors, the colors of shapes can be used for any other purpose depending on the applications and users. For example, the colors can be used for representing additional information such as temporal properties or for identifying different keyposes and body parts.

The motion manifold of input motions can be visualized by drawing the keyposes and the shapes of the spatial and orientational volumes of the body parts. However, drawing the shapes of all body parts sometimes makes it harder to see and may not be appropriate, as shown in Figure 1. The user can choose one or a few key timings and body parts on which to focus. In addition, the camera position can also be controlled by the user so that they can choose a point of focus. This makes our method suitable for interactive visualization because the user can freely change the camera position, key timings, and body parts. Moreover, the user can observe the generated shapes in a virtual reality environment with a head-mounted display.

4.2 Selection of Keyposes

Keypose visualization is a common and useful approach to understanding motion [Assa et al. 2005; Yasuda et al. 2008]. However, especially when there are many input motions, displaying all the keyposes of all motions makes it hard to see them. The range of poses at each key timing should be shown by drawing the minimum number of poses, as shown in Figure 2.

To solve this issue, our method chooses a few keyposes from the keyposes of all input motions for each keypose timing. More specifically, one primary keypose p_p and a few secondary keyposes p_{si} are chosen from the keyposes $p_i \in P_s$ from all input motions. The selected keyposes can be drawn as stick figures, as explained in Section 3.

The primary keypose should be the center pose of the all keyposes. Therefore, the keypose for which the sum of distances to other keyposes is the smallest is chosen as the primary keypose. That is,

$$\mathbf{p}_p = \mathrm{argmin}_{\mathbf{p}_p} \sum_{\mathbf{p}_i \in K} D(\mathbf{p}_p, \mathbf{p}_i), \tag{1}$$

where $\mathbf{p}_i$ is one keypose in the set of all keyposes K and $D(\mathbf{p}_i, \mathbf{p}_i)$ is the distance function between two poses. The distance is computed as the average distance between all the body parts of the two poses after the position and orientation of the poses are aligned by a transformation matrix $\mathbf{T}$. It is calculated as

$$D(\mathbf{p}_i, \mathbf{p}_j) = \frac{1}{n} \sum_{k \in B} |\mathbf{p}_i^k - \mathbf{T}\mathbf{p}_j^k|, \tag{2}$$

where B is the set of all n body parts and $\mathbf{p}_i^k$ and $\mathbf{p}_j^k$ denote the positions k-th body part in the two poses.

The secondary keyposes should show the boundaries of the keyposes. Therefore, we choose the combination of keyposes $S = \mathbf{p}_{s1}, \cdots, \mathbf{p}_{sm}$ for which the sum of distances to the primary keypose as well as the distances to each other is the largest as the secondary poses.

$$S = \mathrm{argmax}_{S \in K} \{D(\mathbf{p}_i, \mathbf{p}_p) + \sum_{\mathbf{p}_i, \mathbf{p}_j \in S} D(\mathbf{p}_i, \mathbf{p}_j)\} \tag{3}$$

Finding such a combination of secondary poses $S \in K$ is considered to be a NP-hard problem. However, as long as the numbers of n and m are small (particularly m), the computational speed is not a problem in our experiments, even with a brute-force approach. If the numbers n and m become large, some approximation and/or optimization algorithms can be introduced for facilitating the process, although this is not explored in this paper.

The number of secondary poses m can be either specified by the user or determined based on a specified threshold for the sum of distances in Equation 3. In our experiments, we took the former approach and used $m = 2$, because determining an appropriate threshold is not straightforward. As a result, three poses were chosen for each of the three key timings in our results (Figures 1 and 2).

4.3 Generation of Spatial Volumes

A series of time-varying positions of a body part in a motion can be represented by a trajectory. However, drawing the trajectories from all input motions makes it hard to see the range of all trajectories, as shown in Figure 3 (a). To solve this issue, our method generates a geometrical shape that contains the trajectories from all input motions for each body part, as shown in Figure 3 (b).

It generates a surface such that the distance to the closest trajectory is a constant value. The distance function is defined by the minimum distance to the closest sample points on all the trajectories. That is,

$$V(\mathbf{p}) = \mathrm{min}_{\mathbf{p}_{ij} \in P} |\mathbf{p} - \mathbf{p}_{ij}|, \tag{4}$$

where $\mathbf{p}$ is an arbitrary point in the space and $\mathbf{p}_{ij}$ is j-th point of i-th trajectory in all sample points P.

To generate a surface, we employ the marching cubes method [Lorensen and Cline 1987], which is a conventional method for surface generation defined by a distance function. It generates a surface by connecting the faces generated for each small voxel in a 3D grid. In our experiments, the size of voxel is set to 0.05 m and the surface distance is set to 0.05 m.

Because the trajectories are represented by a series of positions, the generated surface may become bumpy, especially when the distances between adjacent sample points are large. As postprocessing,

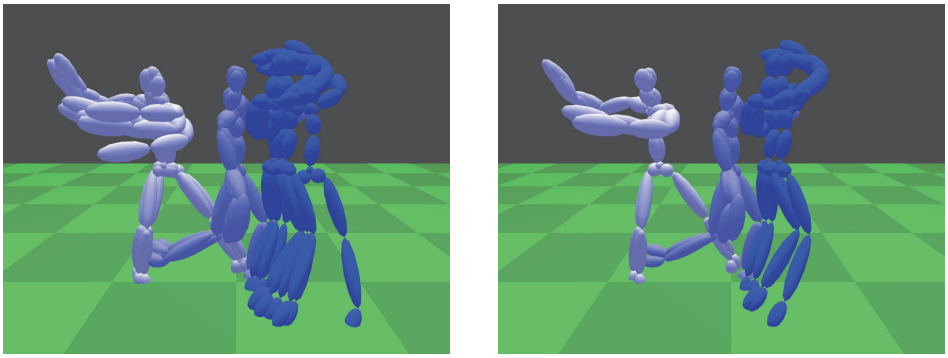

(a) all key poses (b) selected key poses

Figure 2: Selection of keyposes. (a) Input: all example poses for three key timings. (b) Output: selected poses for three key timings.

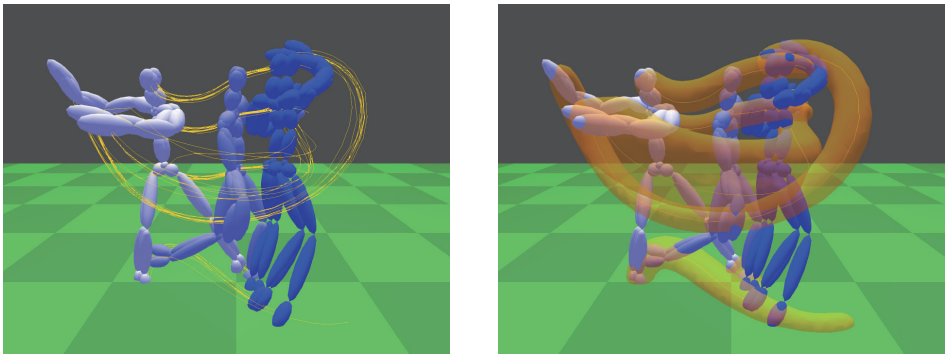

(a) spatial trajectories (b) spatial volumes and center trajectories

Figure 3: Spatial volumes. (a) Input: trajectories for the body parts from all motions. (b) Output: geometrical shapes for the body parts.

we apply a Laplacian smoothing [Sorkine et al. 2004] to make the generated shape smoother.

Although it is possible to use a meta-ball [Blinn 1982] instead of the simple distance function for generating a smoother surface, it is difficult to adjust the distances between adjacent sample points. Therefore, we chose to use a combination of the marching cubes method and Laplacian smoothing.

4.4 Representation of an Orientation

In addition to the positions of a body part, its orientations are also important for understanding its motion. Visualizing a set of orientations is more difficult than visualizing a set of positions. Displaying poses is not enough to show the orientations of the body parts, especially with stick figures, which do not show the rotations of body parts.

Various methods have been used to depict orientations. An arrow (Figure 4 (b)) is a common way to represent an orientation. However, it cannot represent 3D orientation, because the rotation along the direction of arrow cannot be represented. Using three perpendicular arrows to indicate the local coordinates (Figure 4 (c)) is also a common way for representing a 3D orientation. However, this is not suitable for representing many orientations and requires different colors for the three arrows. Although it is also possible to represent a orientational trajectory using a color coded trajectory [Pęszor et al. 2014], this is not very intuitive. Moreover, because the colors often indicate additional information, as mentioned in Section 4.1, using color coding for orientations is not desirable.

To solve the problems of these previous approaches, we introduce flat arrows to represent a 3D orientation in a simple form (Figure 4 (a)). The rotation along the direction of an arrow can also be represented using this flat arrow. Although we can use two different colors for the front and back of a flat arrow to represent 360-degree rotations around the direction of arrow, this is not necessary when only 180 degrees of rotation is sufficient.

To draw a flat arrow, the local coordinates (i.e., the forward-facing axis and upward axis) must be defined for each body part.

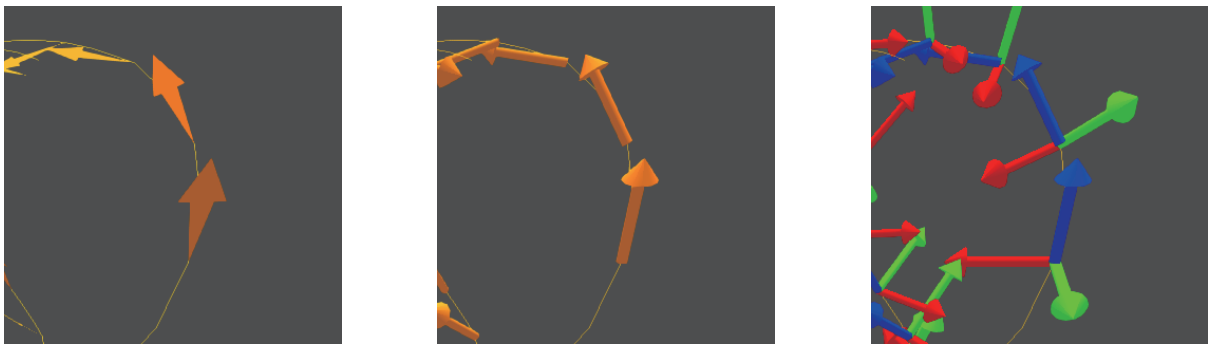

(a) flat arrow representing orientation (our method) (b) arrow representing one direction (c) three arrows representing the local coordinates

Figure 4: Visualization of an orientation. (a) Using flat arrows, our method represents 3D orientation in a simple form. (b) An arrow represents only one direction. (c) Three arrows represent the local coordinates (a 3D orientation).

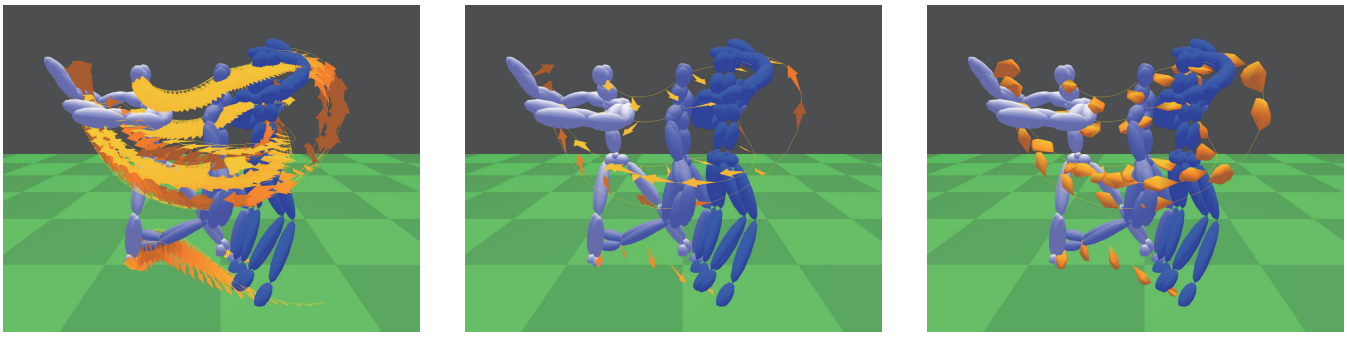

(a) orientations and trajectories (b) selected orientations and center trajectories (c) orientatoinal volume and center trajectories

Figure 5: Orientational volumes. (a) Input: all trajectories with orientations. (b) Center trajectories with orientations. (c) Center trajectories with orientational volumes.

In our experiments, we assigned these axes based on the forward-facing and upward directions of the body parts in an initial T-stance pose.

4.5 Generation of Orientational Volumes

Time-varying orientations can be displayed by drawing the flat arrows on the trajectory at certain intervals, as shown in Figures 5 (a) and (b). Figure 5 (a) shows all trajectories and their orientations, whereas Figure 5 (b) shows the center trajectory and its orientations. The center trajectory for a body part is determined by choosing one trajectory from the trajectories of all input motions. We choose the trajectory with the minimum distance to the position of the body part of the primary keypose over all key frames.

Visualizing a range of orientations is more difficult than visualizing a range of positions. Our method generates a convex hull for the orientations to represent their range. A convex hull is a geometrical shape that contains all sample points, and many algorithms have been developed for computing the convex hull [Berg et al. 2008]. Because the convex hull of a flat arrow contains four vertices, as shown in Figure 4 (a), a convex hull is generated from all the vertices of the flat arrows for the orientations that are collected from all trajectories and associated with the sample point, as shown in Figure 5 (c).

A generated convex hull represents the variation in 3D orientation in a simple form. Our approach works well as long as the variation in orientation is not too large. When it becomes too large, the convex hull also increases, which makes it difficult to present the orientations.

5 EXPERIMENTAL RESULTS

In this section, we present some experimental results of our visualization. We applied our method to tennis shot forms. Our method visualizes the manifold of a set of motions, and it can be used to compare the manifold of a set of motions and the manifold of a single motion. It can also be used to compare the manifold of a set of motions and the manifold of another set of motions.

5.1 Training of Tennis Motion Forms

As mentioned in Section 1, when a trainee would like to practice a form in sport or dance, he or she needs to understand the manifold of the motion form and the differences between this form and

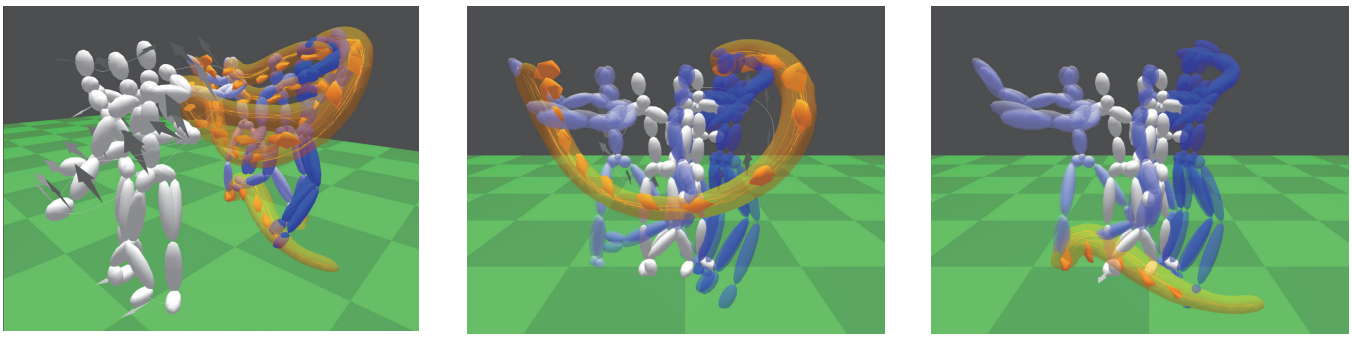

(a) motion volumes of whole body (b) motion volumes of the right hand (c) motion volumes of the right foot

Figure 6: Comparison of the motion volumes of a skilled player (blue poses and orange volumes) and with the motion volumes of a trainee (white poses and gray volumes).

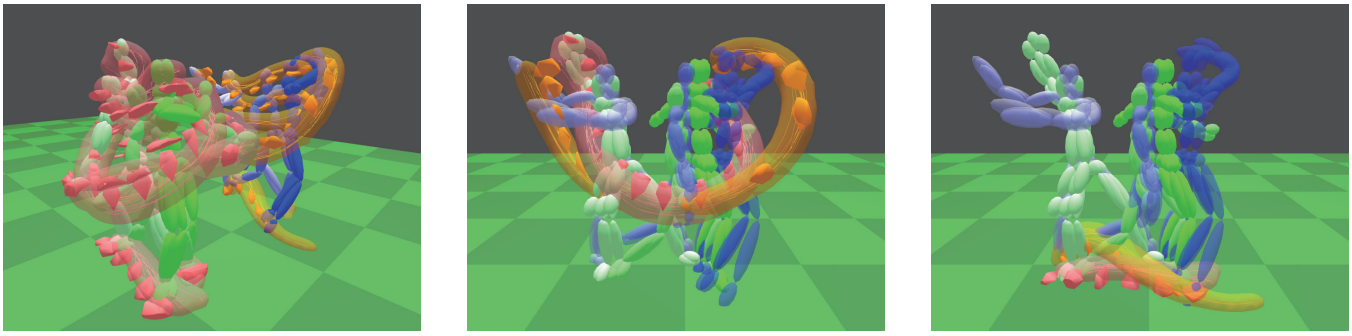

(a) motion volumes of whole body (b) motion volumes of the right hand (c) motion volumes of the right foot

Figure 7: Comparison of the motion volumes of two different skilled players. First player (blue poses and orange volumes) and second player (green poses and pink volumes).

their own motions. To evaluate our method in such a scenario, we visualized the manifold of a tennis forehand shot form and compared it with a trainee's motion. We asked a skilled tennis player to perform forehand shots and captured them using an optical motion-capture system with 12 cameras [Natural Point 2013]. The manifold of the forehand shot was constructed using eight captured motions. We asked a novice trainee with a physique similar to that of the skilled player to perform the forehand shots by mimicking the motion of the skilled player, which was shown as a reference.

A comparison between the motion volumes of the skilled player and that of the trainee is shown in Figure 6. The motion volumes were generated for seven body parts including the pelvis, chest, head, right and left hands, and right and left feet. In Figure 6 (a), the two manifolds are placed at different positions in parallel, because placing them at the same position makes it difficult to see all motion volumes. The trainee's motion is visualized by the keyposes as well as the spatial and orientational trajectories of the body parts. In Figures 6 (b) and (c), they are placed in the same position and the motion volumes of a selected body part are visualized. We can see some deviations of the trainee's motion from the range of the target motion. For example, the trajectory the right hand of the trainee's motion deviated substantially from the spatial volumes of the skilled player in the take-back (initial) and follow-through (terminal) parts of the forehand shots, whereas they are close to each other in the impact (middle) part of the motion. There is a deviation in the orientation of the right hand throughout the entire motion. In addition, the movements of the trainee's right foot are very short compared with the foot movements of the skilled player. In fact, taking a large step is important in the forehand shot form. This visualization shows the problems in the trainee's motion. These findings would help a trainee to understand the problems with his or her motion and fix them.

5.2 Comparison of Tennis Motion Forms

Our method can also be used to compare the manifold of one set of motions with the manifold of another set of motions. We collected 11 motions of the same forehand shots from another skilled player and compare the two sets of motion volumes in Figure 7.

Although they are basically similar, we can see some differences between them. For example, there are difference between the ranges of the right hand in the take-back (initial) and follow-through (terminal) parts of the forehand shots. These findings would be helpful

for understanding the characteristics of the forms of individual players and analyzing them.

5.3 Computational Efficiency

Although our method includes some computationally expensive processes such as computational geometry and combinatorial optimization, in practice, the computational efficiency is not a problem as long as the number of input motions is adequate. In our experiments, all motion volumes of seven body parts for each set of motions were generated within a few seconds on a standard desktop PC (Intel Core i7-8700 3.2 GHz CPU and 16 GB memory). It took 0.16 s for the set of eight motions presented in Section 5.1 and 3.57 s for the set of 11 motions presented in Section 5.2. A further analysis of the computational efficiency in different cases and the optimization of our algorithm are future tasks.

6 DISCUSSION

In this session, we discuss the limitations of our method and future work. One of the limitations is that our method does not visualize temporal information, as mentioned in Section 4.1. Although it is possible to visualize spatial or rotational velocity using additional arrows, the ranges of spatial and/or rotational velocities are difficult to depict in a way that people can easily grasp. Adding a visualization of temporal information is a future task.

Because our method generates a shape that contains all examples, it may be affected by noise, i.e. some motions that deviate from the manifold. If the input dataset contains such noise, some preprocessing for removing noisy samples or post-processing for smoothing the generated geometry may be necessary.

Another limitation is that motion volumes and keyposes may overlap and make it difficult to see when the motions are performed in place and have small translations, because these shapes and keyposes are placed based on their positions with respect to the original motions. This issue can be solved by deforming shapes and placing keyposes in translated positions by scaling them according to the sample times.

Our method does not control the viewing point and direction; they are defined by the user, as mentioned in Section 4.1. Finding the important points in motion volumes where the difference between two manifolds is large and suggesting appropriate viewing points for them may be helpful. This is also future work.

7 CONCLUSION

In this paper, we proposed a method for visualizing the manifold of human motions. Our method visualizes the ranges of time-varying positions and orientations of a body part by generating volumetric shapes for representing them. Our method can help a user to understand the motion manifold of a set of motions as well as the difference between two manifolds. Our future work includes the extension of our method to visualizing temporal information, preprocessing and postprocessing for handling noisy samples, warping shapes and keyposes for avoiding overlaps, and suggesting appropriate viewing points. The application of our method to various kinds of motion forms will also be investigated.

ACKNOWLEDGMENTS

This work was supported in part by Grant-in-Aid for Scientific Research (No. 15H02704) from the Japan Society for the Promotion of Science (JSPS).

REFERENCES

Jackie Assa, Yaron Caspi, and Daniel Cohen-Or. 2005. Action synopsis: pose selection and illustration. *ACM Transactions on Graphics* 24, 3 (2005), 667–676.

Seongmin Baek, Seungyong Lee, and Gerard Jounghyun Kim. 2003. Motion retargeting and evaluation for VR-based training of free motions. *The Visual Computer* 19, 4 (2003), 222–242.

Mark De Berg, Otfried Cheong, Marc van Kreveld, and Mark Overmars. 2008. *Computational Geometry: Algorithms and Applications.* Springer-Verlag Berlin Heidelberg.

James F. Blinn. 1982. A Generalization of Algebraic Surface Drawing. *ACM Transactions on Graphics* 1, 3 (1982), 235–256.

Simon Bouvier-Zappa, Victor Ostromoukhov, and Pierre Poulin. 2007. Motion cues for illustration of skeletal motion capture data. In *International Symposium on Non-Photorealistic Animation and Rendering (NPAR) 2007.* 133–140.

James E. Cutting. 2002. Representing motion in a static image: constraints and parallels in art, science, and popular culture. *Perception* 31 (2002), 1165–1193.

Yueqi Hu, Shuangyuan, Shihong Xia, Jinghua Fu, and Wei Chen. 2010. Motion track: Visualizing variations of human motion data. In *IEEE Pacific Visualization Symposium (PacificVis) 2010.* 152–160.

Sujin Jang, Niklas Elmqvist, and Karthik Ramani. 2014. GestureAnalyzer: visual analytics for pattern analysis of mid-air hand gestures. In *ACM symposium on Spatial user interaction (SUI) 2014.* 30–39.

Rubaiat Habib Kazi, Tovi Grossman, Cory Mogk, Ryan Schmidt, and George Fitzmaurice. 2016. ChronoFab: Fabricating Motion. In *CHI Conference on Human Factors in Computing Systems (CHI) 2016.* 908–918.

Manfred Lau, Ziv Bar-Joseph, and James Kuffner. 2009. Modeling spatial and temporal variation in motion data. *ACM Transactions on Graphics (TOG)* 29, 4 (2009), 171:1–10.

William Li, Lyn Bartram, and Philippe Pasquier. 2016. Techniques and Approaches in Static Visualization of Motion Capture Data. In *International Symposium on Movement and Computing (MoComp) 2016.* 11:1–8.

William E. Lorensen and Harvey E. Cline. 1987. Marching cubes: A high resolution 3D surface construction algorithm. *Computer Graphics* 21, 4 (1987), 163–169.

Jianyuan Min, Yen-Lin Chen, and Jinxiang Chai. 2009. Interactive generation of human animation with deformable motion models. *ACM Transactions on Graphics (TOG)* 29, 1 (2009), 9:1–10.

Natural Point. 2013. Optitrack Motive. http://www.naturalpoint.com/.

Masaki Oshita, Takumi Inao, Shunsuke Ineno, Tomohiko Mukai, and Shigeru Kuriyama. 2019. Development and Evaluation of a Self-Training System for Tennis Shots with Motion Feature Assessment and Visualization. *The Visual Computer* (2019), 1–13.

Damian Pęszor, Dominik Małachowski, Aldona Drabik, Jerzy Paweł Nowacki, Andrzej Polański, and Konrad Wojciechowski. 2014. New Tools for Visualization of Human Motion Trajectory in Quaternion Representation. In *Asian Conference on Intelligent Information and Database Systems 2014.* 152–160.

Yasuhiko Sakamoto, Shigeru Kuriyama, and Toyohisa Kaneko. 2004. Motion map: image-based retrieval and segmentation of motion data. In *ACM SIGGRAPH/Eurographics Symposium on Computer Animation (SCA) 2004.* 159–266.

Yijun Shen, He Wang, Edmond S.L. Ho, Longzhi Yang, and Hubert P.H. Shum. 2017. Posture-based and action-based graphs for boxing skill visualization. *Computers & Graphics* 69 (2017), 104–115.

Yijun Shen, Longzhi Yang, Edmond S.L. Ho, and Hubert P.H. Shum. 2019. Interaction-based Human Activity Comparison. *IEEE Transactions on Visualization and Computer Graphics* (2019), 1–16.

Olga Sorkine, Daniel Cohen-Or, Yaron Lipman, Marc Alexa, Christian Roessl, and Hans-Peter Seidel. 2004. Laplacian Surface Editing. In *Symposium on Geometry Processing (SGP) 2004.* 179–188.

Hiroshi Yasuda, Ryota Kaihara, Suguru Saito, and Masayuki Nakajima. 2008. Motion Belts: Visualization of Human Motion Data on a Timeline. *IEICE Transactions on Information and Systems* E91.D, 4 (2008), 1159–1167.

Xiuming Zhang, Tali Dekel, Tianfan Xue, Andrew Owens, Qiurui He, Jiajun Wu, Stefanie Mueller, and William T. Freeman. 2018. MoSculp: Interactive Visualization of Shape and Time. In *Proceedings of the 31st Annual ACM Symposium on User Interface Software and Technology (UIST '18).* ACM, New York, NY, USA.